

Impact of Molecular Hydrogen on Chalcopyrite Bioleaching by the Extremely Thermoacidophilic Archaeon *Metallosphaera sedula*[∇]

Kathryne S. Auernik and Robert M. Kelly*

Department of Chemical and Biomolecular Engineering, North Carolina State University, Raleigh, North Carolina 27695-7905

Received 21 August 2009/Accepted 16 February 2010

Hydrogen served as a competitive inorganic energy source, impacting the CuFeS₂ bioleaching efficiency of the extremely thermoacidophilic archaeon *Metallosphaera sedula*. Open reading frames encoding key terminal oxidase and electron transport chain components were triggered by CuFeS₂. Evidence of heterotrophic metabolism was noted after extended periods of bioleaching, presumably related to cell lysis.

For bioleaching processes focused on the recovery of base, precious, and strategic metals from low-grade ores, most microorganisms studied to date are mesophilic bacteria (18). However, moderately and extremely thermoacidophilic archaea may be advantageous in certain bioleaching applications and should be considered (7, 8; T. Harvey and W. van der Merwe, presented at the Bio & Hydrometallurgy Meeting, Capetown, South Africa, 2002). For chalcopyrite (CuFeS₂) bioleaching, for example, higher temperatures can lead to faster overall leaching kinetics, in part by minimizing passivation, which slows rates at the mineral surface (15, 16). *Metallosphaera sedula*, an extremely thermoacidophilic, metal-mobilizing crenarchaeon growing optimally at 70 to 75°C and pH 2 (3), has been examined in this regard (7, 11). Key to bioleaching capacity in this microorganism is the dissimilatory oxidation of iron and sulfur, mediated by membrane-associated electron transport chains that are anchored by terminal oxidases (2, 3, 12). For *M. sedula*, another factor that needs to be considered is the impact of inorganic energy sources, other than metal sulfides, on bioleaching. This issue was considered here by examining the influence of molecular hydrogen on *M. sedula* CuFeS₂ bioleaching.

M. sedula (DSMZ 5348) was grown aerobically at 70°C in an orbital bath (70 rpm). Autotrophic cultures (headspace content: 7% CO₂, 14% O₂, 28% H₂, balance N₂) were used to inoculate 1-liter bottles containing 300 ml of DSMZ medium 88 (pH 2), supplemented with 10 g/liter chalcopyrite (provided by Greg Olsen [Geosynfuels, Golden, CO]), and a headspace of either air, air plus CO₂ (7% final concentration), or the autotrophic mix mentioned above. Cells were enumerated using epifluorescence microscopy with acridine orange stain. Cultures growing exponentially were harvested 1 day postinoculation and compared to CuFeS₂-grown cultures that were harvested 3 or 9 days postinoculation. Harvesting was done as previously described (2, 3). Methods used for microarray construction, RNA preparation, slide scanning, and data analysis were also as described previously, with the exception that

Trizol (Invitrogen) was used as the RNA extraction reagent and a Packard BioChip Scanarray 4000 scanner was used for slide scanning. Significant differential transcription, or “response,” was defined as relative changes of ≥ 2 (where a log₂ value of ± 1 means a 2-fold change) having significance values of ≥ 5.4 (Bonferroni correction equivalent to a *P* value of 4.0×10^{-6} for this microarray configuration). Soluble iron and its oxidation state in *M. sedula* cultures were tracked using an *o*-phenanthroline colorimetric assay modified from ASTM E3934 and reference 14.

Ferric iron precipitation is minimized during bioleaching in the presence of H₂. Chalcopyrite bioleaching in *M. sedula* cultures was compared to that in abiotic controls 9 days postinoculation. Visual inspection of chalcopyrite cultures with an air-only headspace revealed evidence of biotic activity (rust-colored precipitate) compared to their abiotic control. However, no visual evidence of ferric iron formation was evident for cultures growing in an H₂-containing headspace or their abiotic control (Fig. 1A). Measurement of soluble iron (almost entirely in the reduced Fe²⁺ state) for H₂-containing conditions showed accumulation of significantly greater amounts of iron in inoculated cultures than in their abiotic control (Fig. 1B). This indicated that bioleaching also occurred in the H₂-supplemented cultures, despite an absence of ferric iron precipitates typically associated with bioleaching activity. It was unclear how the presence of H₂ correlated with the absence of extensive precipitate formation. The absence of significant amounts of ferric iron in solution for all abiotic controls suggests that the rate of reduction of ferric iron by the Cu-containing bioleaching substrate may be higher than for pyritic substrates without Cu (where significant amounts of ferric iron can exist in solution), which offers an inorganic hypothesis limiting ferric iron availability for precipitate formation in H₂-containing *M. sedula* cultures (where dissolved oxygen concentrations available for precipitate formation are also reduced). An organic hypothesis suggests the possibility of biological coupling of H₂ oxidation to ferric iron reduction (concomitant with the predominant biological oxidation effect observed in Fig. 1B), which would limit ferric iron availability for precipitate formation.

Specific bioleaching rates are negatively impacted by the presence of H₂. To determine the impact of H₂ on specific bioleaching rates, cell density, and total soluble iron were

* Corresponding author. Mailing address: Department of Chemical and Biomolecular Engineering, North Carolina State University, EB-1, 911 Partners Way, Raleigh, NC 27695-7905. Phone: (919) 515-6396. Fax: (919) 515-3465. E-mail: rmkelly@eos.ncsu.edu.

[∇] Published ahead of print on 26 February 2010.

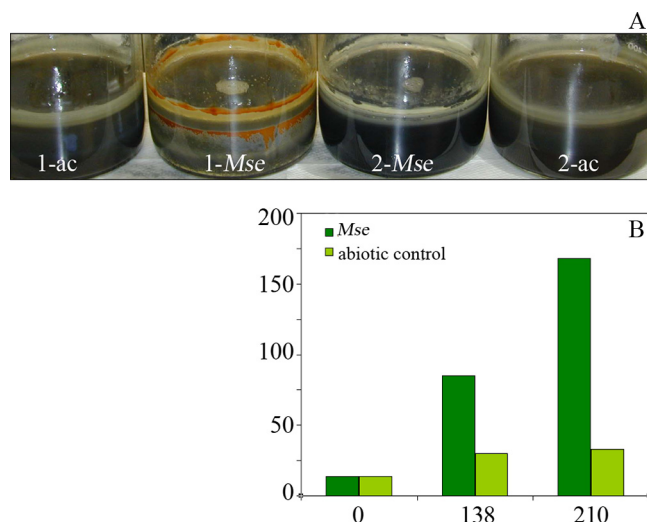


FIG. 1. Chalcopyrite bioleaching by *M. sedula*. (A) Nine days post-inoculation, chalcopyrite bioleaching by *M. sedula* exposed to an air headspace (1-*Mse*) is visually evident compared to its abiotic control (1-*ac*). No obvious evidence of bioleaching is visible for *M. sedula* grown in a hydrogen-containing headspace (2-*Mse*) or the associated abiotic control (2-*ac*). (B) Total soluble iron (mg/liter, measured as a function of hours postinoculation) is significantly higher in cultures containing *M. sedula* grown in a hydrogen-containing headspace than the abiotic control, indicating active bioleaching. Typical standard deviations of <10 mg/liter were found for the iron assay ($n = 3$ for abiotic controls; $n = 9$ for *M. sedula* cultures).

tracked for 6 days following inoculation for *M. sedula* cultures with an air headspace enhanced with H₂+CO₂ or CO₂. Following harvest of CO₂-enhanced cultures (no H₂ present), which had iron precipitate on vessel walls that was similar to that in air-only headspace cultures (no H₂ or CO₂ present [data not shown]), the precipitate adhering to the wall was dissolved using 10 N HCl; the working volumes were then restored to that of the initial culture. The resulting total soluble iron levels were determined, such that the total iron release reported for CO₂-enhanced cultures includes contributions from the precipitate that accumulated on culture vessel walls. It should be noted that 6 days after inoculation, total iron levels in solution were the same for air headspace cultures as for CO₂-enhanced headspace cultures (data not shown); no iron contribution from wall precipitates was included for air-only cultures. Specific bioleaching rates were calculated by dividing the average cell density (note that cells were counted in a two-dimensional space; therefore, cells attached to the bottom of particles would have been missed for both culture conditions) during the 6-day postinoculation period by the total amount of iron released from the chalcopyrite during the same time. The specific leaching rate for H₂+CO₂-enhanced cultures was 5.1×10^{-10} mg Fe/cell compared to 2.8×10^{-9} mg Fe/cell for CO₂-enhanced cultures, or more for the CO₂-enhanced cultures. There was no significant difference in total iron released biotically from H₂+CO₂- or CO₂-enhanced cultures during this period (55 mg/liter versus 62 mg/liter, respectively). However, the difference in average planktonic cell densities (1.1×10^8 cells/ml of H₂-containing culture compared to 2.2×10^7 cell/ml of CO₂-enhanced

culture) indicated that H₂-supplemented cultures were less efficient in bioleaching (total iron release) on a per-cell basis. The higher biomass and faster growth rates in the H₂ + CO₂-enhanced cultures compared to the air-only and CO₂-enhanced cultures indicated that H₂ served as an alternate energy source for *M. sedula*.

Competition between H₂ and Fe²⁺ as energy sources. Components of electron transport chains in *M. sedula* have been examined with respect to iron and sulfur oxidation activities, as this relates to bioleaching capabilities (2, 3). Figure 2 shows these components and their transcriptional response when exposed to chalcopyrite for up to 9 days, and Table 1 provides detailed transcriptomic information.

Components of electron transport chains associated with Fe²⁺-based electron sources were activated upon exposure to chalcopyrite, indicating that Fe²⁺ was being utilized as an energy source. These components included those encoded by *soxNL* and *cbsA'A* (cytochrome *b*), the *foxA* transcript from the *fox* cluster originally described in the iron oxidizer *Sulfolobus metallicus* (5), a putative rusticyanin (Msed_0966), a terminal oxidase (*doxBCE*, Msed_2032, 2031, and 2030) previously described in *Acidianus ambivalens* (17), and a putative pyruvate:ferredoxin oxidoreductase (Pfor $\gamma\delta\alpha\beta$, Msed_0507 to 0510). Consistent with previous observations for growth on soluble iron (2, 3), the *soxNL-cbsA'A* transcripts were all significantly upregulated in the presence of chalcopyrite (day 9) compared to the inoculum (day 0). While the *foxA'BCD* (Msed_0485, 0480, 0478, and 0477) transcripts were downregulated in the presence of chalcopyrite (day 9 versus day 0), the *foxA* (Msed_0484) transcript was upregulated after exposure to chalcopyrite (day 3 versus day 0). This suggests that the utility of FoxAA'BCD for electron transport from Fe²⁺ correlates with activation of the *foxA* and downregulation of *foxA'* transcripts. Of particular note is the 10.5-fold ($P = 2.3 \times 10^{-6}$) upregulation of *rus* (Msed_0966; day 9 versus day 0); the putative protein encoded in this open reading frame ORF, a rusticyanin homolog, has been implicated in electron transfer from Fe²⁺ in the model mesophilic bioleaching organism *Acidithiobacillus ferrooxidans* (19). Here, maximum soluble iron levels were <0.2 g/liter, significantly lower than the soluble iron levels from previous *M. sedula* studies (2.7 to 3.7 g Fe/liter) in which no significant differential transcription of *rus* was reported. Thus, transcription of this *M. sedula* gene may be triggered by additional factors beyond soluble iron levels.

Downstream of *pfor*, the gene encoding a putative pyruvate synthase converting acetyl coenzyme A (acetyl-CoA) from inorganic carbon fixation into pyruvate using electrons from reduced ferredoxin (3a), are several hypothetical proteins (Msed_0511, 0512, and 0515) that are homologs (24 to 32% identity) of bacterial PqqE proteins implicated in pyrroloquinoline quinone cofactor biosynthesis (9, 10, 13) and a hypothetical protein (Msed_0518) similar to several uncharacterized flavoproteins. As was previously noted on soluble iron, these ORFs were upregulated on chalcopyrite (Table 1).

Hydrogenase accessory and maturation transcripts did not respond differently to the growth conditions studied here, although both the α subunit (Msed_0945) and the membrane anchor (Msed_0946) of the primary hydrogenase were downregulated from day 3 to day 9. Despite this response, transcripts for the hydrogenase genes were still highly transcribed

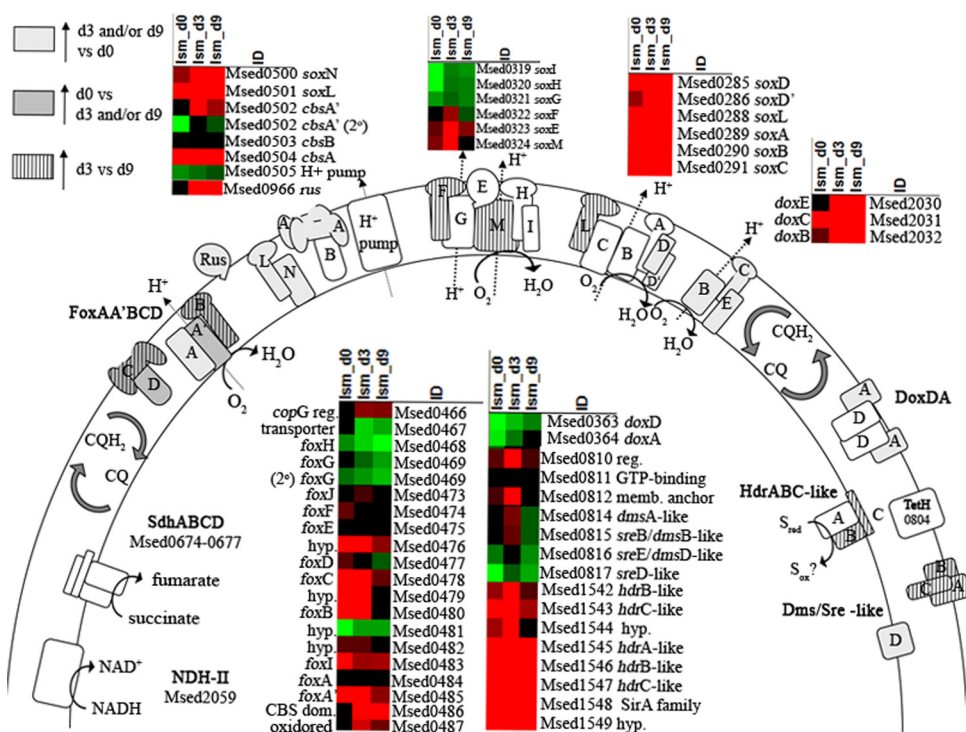


FIG. 2. Heat plot of electron transfer components involved with oxidation of Fe(II) and RISCs. Heat plots were compiled using Array File Maker 4.0 (6). Red indicates levels of high transcription, black indicates average transcription (set to an LSM [least squares mean of normalized \log_2 transcription levels] of 0), and green indicates levels of low transcription, for *M. sedula* ORFs in the inoculum (d0), at 3 days of growth on CuFeS_2 (d3), and at 9 days of growth on CuFeS_2 (d9).

at day 9. This indicates that while H_2 was no longer the primary energy source, *M. sedula* was still deriving bioenergetic benefit from molecular hydrogen. The heterodisulfide-like cluster (Msed_1542 to 1549), which is likely involved in electron transfer from hydrogenases (3a) and reduced inorganic sulfur compounds (RISCs) (2), was highly transcribed here; unlike the hydrogenase structural components, it did not change from day 3 to 9. Transcripts for the *soxABCDD'* terminal oxidase, activated when exposed to either RISCs or H_2 , were differentially transcribed when exposed to chalcopyrite. The ORF encoding *soxDD'* (Msed_0285/Msed_0286) was upregulated upon exposure to chalcopyrite, and transcripts for the Rieske protein, encoded by *soxL* (Msed_0288), were downregulated from day 3 to day 9. A putative sulfide:quinone reductase (Msed_1039, *sqr*-like), predicted to be targeted to the outside of the membrane by both SignalP and the archaeal PRED-SIGNAL (3, 4), was upregulated 3.4-fold ($P = 6.3 \times 10^{-10}$) from day 3 to 9. The downregulation of several hydrogenase components, combined with the upregulation of several ORFs possibly involved in sulfur oxidation and lack of response from the *hdr*-like cluster thought to utilize both energy sources, suggests that RISCs may also be serving as an inorganic energy source by day 9.

Although it is clear that the inoculum used for chalcopyrite cultures was growing autotrophically on inorganic carbon and H_2 , it is unclear what growth mode(s) characterizes growth on chalcopyrite. Multiple inorganic energy sources are available—chalcopyrite provided a source of Fe^{2+} and RISCs, in addition

to the H_2 present in the headspace. Once the culture is in stationary phase, a potential source of organic carbon (and possibly an energy source) is proteins and peptides released through cell lysis. Several transcripts encoding enzymes of the 3-hydroxypropionate/4-hydroxybutyrate cycle of inorganic carbon fixation were highly transcribed at day 0 and day 3, but transcription decreased by day 9: the putative carbonic anhydrase (Msed_0390), acetyl-/propionyl-CoA carboxylase (Msed_0147, 0148, and 1375), and malonyl-/succinyl-CoA reductase (Msed_0709). This suggested that *M. sedula* switched away from inorganic carbon fixation, most likely in favor of an organic carbon source, a strong preference based on previous mixotrophy studies (3a). This is further supported by upregulation of several transcripts associated with TCA (tricarboxylic acid) intermediate cycling (Msed_1581/Msed_1582), aromatic amino acid catabolism (Msed_1772–Msed_1777), and removal of excess N from organic carbon substrates (Msed_2074) (data not shown). It is not clear if this organic carbon also serves as a competitive energy source, but it has the potential to negatively impact inorganic energy utilization by reducing inorganic carbon fixation.

While supplementing *M. sedula* bioleaching cultures with H_2 offers a method to build biomass and reduce potentially undesirable ferric iron compound precipitation, it also reduces specific bioleaching rates (both directly and indirectly). Further studies are needed to understand the energy metabolism of *M. sedula* (and related extreme thermoacidophiles) in order to optimize their function as bioleaching agents (1).

TABLE 1. Transcriptional response for inorganic energy source utilization

Category/function	ORF	Annotation	Change (<i>n</i> -fold)	Time point comparison (days)
Iron oxidation	Msed_0467	Transporter	+6.8	0 vs 9
	Msed_0469	<i>foxG</i>	+3.8	0 vs 9
	Msed_0477	<i>foxD</i>	+6.3	0 vs 9
	Msed_0478	<i>foxC</i>	+5.8	0 vs 9
	Msed_0479	Unique hypothetical protein (80 aa)	+15.1	0 vs 9
	Msed_0480	<i>foxB</i>	+12.5	0 vs 9
	Msed_0484	<i>foxA</i>	-3.0	0 vs 3
	Msed_0485	<i>foxA'</i>	+5.1	0 vs 9
	Msed_0486	CBS domain	-11.5	0 vs 9
	Msed_0500	<i>soxN</i>	-3.0	0 vs 9
	Msed_0501	<i>soxL2</i>	-4.7	0 vs 3
	Msed_0502	<i>cbsA'</i>	-3.6	0 vs 9
	Msed_0504	<i>cbsA</i>	-3.2	0 vs 9
	Msed_0966	<i>rus</i>	-10.5	0 vs 9
Fe/inorganic electron transport	Msed_0510	<i>pfor</i> β	-3.7	0 vs 3
	Msed_0511	<i>pqqE</i> -like	-15.5	0 vs 3
	Msed_0512	<i>pqqE</i> -like	-24.3	0 vs 3
	Msed_0513	Conserved hypothetical	-20.0	0 vs 3
	Msed_0514	U32 peptidase	-18.7	0 vs 3
	Msed_0515	<i>pqqE</i> -like	-6.0	0 vs 3
	Msed_0516	Conserved hypothetical	-6.4	0 vs 3
Fe oxidation/S oxidation	Msed_2030	<i>doxE</i>	-11.4	0 vs 9
	Msed_2031	<i>doxC</i>	-2.4	0 vs 9
	Msed_2032	<i>doxB</i>	-5.1	0 vs 9
	Msed_0570	<i>doxB2</i>	-3.7	0 vs 9
	Msed_1039	<i>sqr</i> -like	-3.4	0 vs 9
	Msed_0364	<i>doxA</i>	-3.1	0 vs 9
S oxidation/H ₂ utilization	Msed_0285	<i>soxD</i>	-2.5	0 vs 3
	Msed_0286	<i>soxD'</i>	-3.0	0 vs 3
	Msed_0288	<i>soxL</i>	+2.4	3 vs 9
H ₂ utilization	Msed_0945	<i>hynL</i>	+4.7	3 vs 9
	Msed_0946	<i>isp1</i>	+3.6	3 vs 9
	Msed_0948	Conserved hypothetical	+4.4	3 vs 9
	Msed_0949	Conserved hypothetical	+3.9	3 vs 9
Inorganic carbon fixation	Msed_0390	Carbonic anhydrase	+3.4	3 vs 9
	Msed_0147	Acetyl-/propionyl-CoA carboxylase	+5.6	3 vs 9
	Msed_0148	Acetyl-/propionyl-CoA carboxylase	+3.3	3 vs 9
	Msed_1375	Acetyl-/propionyl-CoA carboxylase	+4.7	3 vs 9
	Msed_0709	Malonyl-/succinyl-CoA reductase	+5.7	3 vs 9

Transcriptional response data accession number. Transcriptional response data are available through the NCBI Gene Expression Omnibus (GEO) database under accession number GSE 20554.

We thank Greg Olson for providing the chalcopyrite used in this work. K.S.A. acknowledges support from the NCSU Molecular Biotechnology Training Program through an NIH T32 Biotechnology Traineeship. R.M.K. acknowledges support from the NSF Biotechnology Program and from the U.S. Defense Threat Reduction Agency (DTRA).

REFERENCES

- Auernik, K. S., C. R. Cooper, and R. M. Kelly. 2008. Life in hot acid: pathway analyses in extremely thermoacidophilic archaea. *Curr. Opin. Biotechnol.* **19**:445–453.
- Auernik, K. S., and R. M. Kelly. 2008. Identification of components of electron transport chains in the extremely thermoacidophilic crenarchaeon *Metallosphaera sedula* through iron and sulfur compound oxidation transcriptomes. *Appl. Environ. Microbiol.* **74**:7723–7732.
- Auernik, K. S., Y. Maezato, P. H. Blum, and R. M. Kelly. 2008. The genome sequence of the metal-mobilizing, extremely thermoacidophilic archaeon *Metallosphaera sedula* provides insights into bioleaching-associated metabolism. *Appl. Environ. Microbiol.* **74**:682–692.
- Auernik, K. S., and R. M. Kelly. 2010. Physiological versatility of the extremely thermoacidophilic archaeon *Metallosphaera sedula* supported by heterotrophy, autotrophy, and mixotrophy transcriptomes. *Appl. Environ. Microbiol.* **76**:931–935.
- Bagos, P. G., K. D. Tsirigos, S. K. Plessas, T. D. Liakopoulos, and S. J. Hamodrakas. 2009. Prediction of signal peptides in archaea. *Protein Eng. Des. Sel.* **22**:27–35.
- Bathe, S., and P. R. Norris. 2007. Ferrous iron- and sulfur-induced genes in *Sulfolobus metallicus*. *Appl. Environ. Microbiol.* **73**:2491–2497.
- Breitkreutz, B. J., P. Jorgensen, A. Breitkreutz, and M. Tyers. 2001. AFM 4.0: a toolbox for DNA microarray analysis. *Genome Biol.* **2**:SOFTWARE0001.
- Clark, T. R., F. Baldi, and G. J. Olson. 1993. Coal depyritization by the thermophilic archaeon *Metallosphaera sedula*. *Appl. Environ. Microbiol.* **59**:2375–2379.
- Du Plessis, C. A., J. D. Batty, and D. W. Dew. 2007. Commercial applications of thermophile bioleaching. In D. E. Rawlings and D. B. Johnson (ed.), *Biomining*. Springer-Verlag, Berlin, Germany.
- Felder, M., A. Gupta, V. Verma, A. Kumar, G. N. Qazi, and J. Cullum. 2000. The pyrroloquinoline quinone synthesis genes of *Gluconobacter oxydans*. *FEMS Microbiol. Lett.* **193**:231–236.
- Goosen, N., H. P. Horsman, R. G. Huinen, A. de Groot, and P. van de Putte.

1989. Genes involved in the biosynthesis of P from *Acinetobacter calcoaceticus*. *Antonie Van Leeuwenhoek* **56**:85–91.
11. Han, C. J., and R. M. Kelly. 1998. Biooxidation capacity of the extremely thermoacidophilic archaeon *Metallosphaera sedula* under bioenergetic challenge. *Biotechnol. Bioeng.* **58**:617–624.
 12. Kappler, U., L. I. Sly, and A. G. McEwan. 2005. Respiratory gene clusters of *Metallosphaera sedula*—differential expression and transcriptional organization. *Microbiology* **151**:35–43.
 13. Meulenber, J. J., E. Sellink, N. H. Riegman, and P. W. Postma. 1992. Nucleotide sequence and structure of the *Klebsiella pneumoniae* p operon. *Mol. Gen. Genet.* **232**:284–294.
 14. Muir, M., and T. Andersen. 1977. Determination of ferrous iron in copper-process metallurgical solutions by the o-phenanthroline colorimetric method. *Metallurgical Transactions B Process Metallurgy* **8B**:517–518.
 15. Norris, P. R., N. P. Burton, and N. A. Foulis. 2000. Acidophiles in bioreactor mineral processing. *Extremophiles* **4**:71–76.
 16. Olson, G. J., J. A. Brierley, and C. L. Brierley. 2003. Bioleaching review part B: progress in bioleaching: applications of microbial processes by the minerals industries. *Appl. Microbiol. Biotechnol.* **63**:249–257.
 17. Purschke, W. G., C. L. Schmidt, A. Petersen, and G. Schafer. 1997. The terminal quinol oxidase of the hyperthermophilic archaeon *Acidianus ambivalens* exhibits a novel subunit structure and gene organization. *J. Bacteriol.* **179**:1344–1353.
 18. Valdes, J., I. Pedroso, R. Quatrini, R. J. Dodson, H. Tettelin, R. Blake, 2nd, J. A. Eisen, and D. S. Holmes. 2008. *Acidithiobacillus ferrooxidans* metabolism: from genome sequence to industrial applications. *BMC Genomics* **9**:597.
 19. Yarzabal, A., C. Appia-Ayme, J. Ratouchniak, and V. Bonnefoy. 2004. Regulation of the expression of the *Acidithiobacillus ferrooxidans rus* operon encoding two cytochromes c, a cytochrome oxidase and rusticyanin. *Microbiology* **150**:2113–2123.